On the temperature dependence of the ionization potential of self-compressed solid- and liquid-metallic clusters

1996 J. Phys.: Condens. Matter 8 4245

(http://iopscience.iop.org/0953-8984/8/23/016)

J. Phys.: Condens. Matter **8** (1996) 4245–4257. Printed in the UK

On the temperature dependence of the ionization potential of self-compressed solid- and liquid-metallic clusters

Adam Kiejna† and Valentin V Pogosov‡§

† Institute of Experimental Physics, University of Wrocław, Plac M Borna 9, 50-204 Wrocław, Poland

‡ Theoretical Department, Institute for High Temperatures, Russian Academy of Sciences, Izhorskaya Street 13/19, 127412, Moscow, Russia

§ Department of Physics, Zaporozhye State Technical University, Zhukovski Street 64, 330063, Zaporozhye, Ukraine

Received 6 February 1996

Abstract. The density functional theory and sum-rule approach are used to calculate the electronic chemical potential of large self-compressed metallic clusters in the stabilized-jellium model and the two-component model that mimic the solid and the liquid state. The ionization potential is defined as the sum of the electronic chemical potential for a neutral cluster, and the ordinary electrostatic contribution $e^2/2R$. Using the analytic expressions derived, the temperature dependencies of the work function and of the term connected with spontaneous deformation have been estimated. The calculations show noticeable size-shrinkage contributions to the ionization potential. In the two-component statistical version of the density functional formalism, substantial changes induced by a transition from cold clusters to the liquid state are observed.

1. Introduction

The size-dependent properties of metallic clusters are of considerable current interest, both experimentally [1–3] and theoretically [4, 5]. Much attention has been paid to the understanding of trends of measured ionization potentials (IP) and electron affinities (EA) of clusters. The analysis of experimental data on these quantities for small metallic particles (clusters) is usually carried out according to the formulae

$$\begin{aligned} \mathrm{IP} &= W_{e0} + \alpha\frac{e^2}{R} + \mathrm{O}(R^{-2}) \\ \mathrm{EA} &= W_{e0} - \beta\frac{e^2}{R} + \mathrm{O}(R^{-2}) \end{aligned} \tag{1}$$

where W_{e0} is the electron work function for a planar surface and R is the cluster radius. The dimensionless coefficients α and β are dominated by the contribution resulting from the classical electrostatics which gives $\alpha = \beta = \frac{1}{2}$ [6]. In experiment one observes deviations from this value which can be ascribed to a quantum defect. A recent review [3] of the available experimental data shows that for clusters of K, Na, Li, Ag, and Al the fitting values for α fall in the range between 0.32 and 0.45. In these analyses no self-compression and temperature effects were taken into consideration.

In the limit $R \to \infty$ the values of IP(R) and EA(R) for the closed-shell clusters should reduce to the observed polycrystalline work functions for zero temperature. This is indeed

0953-8984/96/234245+13$19.50

observed for the simple metals. However, unlike such characteristics of metals as the work function and surface energy, which at least for simple metals are monotonic functions of the electron density, the experimental data on α do not permit any conclusion to be drawn about the nature of the function $\alpha(r_{s0})$. Here r_{s0} is the electron density parameter, $4\pi r_{s0}^3 \bar{n}_0/3 = 1$, and $\bar{n}_0$ is the electron concentration in the bulk.

The calculations performed within various approaches for clusters [7–12] do not give an unequivocal answer about the dependencies of $\alpha(r_{s0})$ and $\beta(r_{s0})$ either. They vary weakly with r_{s0} and fall into the same range of magnitudes: $0.4 \leqslant \alpha(r_{s0}) < 0.5$ and $0.5 < \beta(r_{s0}) \leqslant 0.6$. It should be noted that all of these calculations have been carried out for *rigid* and *cold* clusters within the jellium model. It is well known that the ordinary jellium model exhibits serious deficiencies such as negative surface energy for $r_{s0} \leqslant 2a_0$ and negative bulk modulus for $r_{s0} \geqslant 6a_0$ (a_0 is the Bohr radius). These can be remedied by using the stabilized-jellium model. In the latter model the lattice effects, or electron–ion interactions, are represented in an averaged way, providing a more realistic description of the bulk and surface properties of solid simple metals [13–15]. A calculation of self-compression for Al, Na, and Cs clusters with the valence electron number $N \leqslant 20$ has been performed by Perdew *et al* [16] in the framework of stabilized jellium.

According to a widely accepted point of view [17], for a large radius of the cluster, the IP and EA can be expressed as

$$\begin{aligned} \mathrm{IP} &= -\mu_{e0} + \frac{e^2}{2R} - \frac{\mu_{e1}}{R} + \mathrm{O}(R^{-2}) \\ \mathrm{EA} &= -\mu_{e0} - \frac{e^2}{2R} - \frac{\mu_{e1}}{R} + \mathrm{O}(R^{-2}). \end{aligned} \tag{2}$$

Comparing equations (1) and (2) we see that the quantities α and β denote the curvature corrections to the IP and EA. Accordingly we have: $\alpha = \frac{1}{2} - \mu_{e1}/e^2$, $\beta = \frac{1}{2} + \mu_{e1}/e^2$, and $\mu_e(R) = \mu_{e0} + \mu_{e1}/R$ is the electronic chemical potential for neutral cluster, $\mu_{e0} = -W_{e0}$. The second term, $e^2/2R$, has its origin in electrostatic 'self-interaction' of the surplus unit charge. In the 'thermodynamic limit' the quantum-size correction, μ_{e1}/R, is a very delicate characteristic, and is sensitive to errors in the variational procedure [9].

It should be noted that for experiments on clusters the interpretation of results usually assumes that they are *cold* and *rigid* finite systems. In connection with this observation there are two points worth mentioning: (i) the electron work function (which is an asymptotic limit $R \to \infty$ of the cluster IP) and surface tension of metals depend on the temperature [18–20]; and (ii) the surface tension of a finite system leads to a shrinkage of the Wigner–Seitz density parameter compared to its bulk value.

In this paper, we present calculations, based on a sum-rule approach, for elastic liquid and *hot* solid clusters of simple metals which exhibit spontaneous deformation [17]. The self-compression follows from a condition of mechanical equilibrium for clusters in vacuum. It is well known that flat-surface characteristics of liquid metals strongly depend on temperature [20]. Only a few theoretical investigations have been devoted to the study of the influence of temperature on the size effects within approaches that mimic a liquid state [21–23]. For investigation of thermodynamic properties of metallic clusters we invoke the two-component plasma model which places the 'classical' ions and conduction electrons on an equal footing [19, 20]. This model has been shown to provide a realistic description of surface tension of simple metals over a wide range of temperatures.

The sum-rule approach permits evaluation of size corrections in terms of quantities for a planar surface. We will first present the density functional equations for a two-component liquid metal, which will show the origins of the respective contributions to the size effect.

Then corresponding equations for stabilized jellium are derived. The results of calculations and possible applications are discussed in section 3. Finally, section 4 provides a summary and conclusions.

2. Theory

2.1. The two-component model

For liquid clusters of monovalent alkali metals we employ a version of the density functional theory which starts from the assumption that a statistical description of the electronic subsystem of a cluster applies. The cluster size must be sufficiently large for the concepts of Fermi energy and chemical potential to have meaning. On the other hand, it must be sufficiently small for the size effects to be noticeable. The case considered here is the limit of weak quantization, when the cluster contains hundreds of atoms and the electronic chemical potential is much larger than the mean spacing between the electron energy levels in the cluster.

The free energy of electron–ion plasma of the liquid cluster, $F = F[n_e(\boldsymbol{r}, R), n_i(\boldsymbol{r}, R)]$ is a functional of the inhomogeneous electronic ($n_e(\boldsymbol{r}, R)$) and ionic ($n_i(\boldsymbol{r}, R)$) concentrations. Using a gradient approximation, the free energy can be written in the form

$$F = \int \mathrm{d}^3 r \ \left(f + f_{ee} \, |\nabla n_e|^2 + f_{ei} \nabla n_e \nabla n_i + f_{ii} \, |\nabla n_i|^2 \right) + \frac{e}{2} \int \mathrm{d}^3 r \ \phi(\boldsymbol{r}, R)[n_e(\boldsymbol{r}, R) - n_i(\boldsymbol{r}, R)] \tag{3}$$

where $f \equiv f[n_e(\boldsymbol{r}, R), n_i(\boldsymbol{r}, R)]$ is the energy density of the quasi-homogeneous part of the functional corresponding to the local density approximation, $f_{aa} \equiv f_{aa}(n_e(\boldsymbol{r}, R), n_i(\boldsymbol{r}, R))$ gives the first inhomogeneity term represented by the gradient terms for both electrons and ions ($a = \mathrm{e}, \mathrm{i}$), and ϕ is the electrostatic potential of the system.

The quasi-homogeneous part of the free energy, appearing in the first integral in equation (3), takes into account the following components in the structural expansion in terms of the weak electron–ion interaction described by the Ashcroft pseudopotential: the electron kinetic energy and the exchange–correlation energy in the Nozières–Pines approximation; the Madelung energy owing to the ion–ion interaction; the energy of electron–ion interaction evaluated in the first order of perturbation theory; the band-structure energy; and the entropy of the ideal degenerate electron gas and of the classical system of ions represented by hard spheres. For the explicit forms of these components and of the gradients terms we refer the reader to [20].

For the equilibrium density profiles, $n_e(\boldsymbol{r}, R)$ and $n_i(\boldsymbol{r}, R)$, the functional $\Omega_V[n_e, n_i] = F - \mu_e N_e - \mu_i N_i$ has a minimum and equals the Gibbs grand potential, $\Omega = -PV$, where P is the pressure in a system of volume V, and $\mu_{e,i}$ and $N_{e,i}$ denote the chemical potential and number of particles for electrons and ions, accordingly. Then, we can write out the Euler–Lagrange equations for a two-component plasma of liquid metal:

$$\mu_e(\boldsymbol{r}, R) = +e\phi(\boldsymbol{r}, R) + \delta F / \delta n_e(\boldsymbol{r}, R) \tag{4}$$

$$\mu_i(\boldsymbol{r}, R) = -e\phi(\boldsymbol{r}, R) + \delta F / \delta n_i(\boldsymbol{r}, R) \tag{5}$$

where the electrostatic potential satisfies the Poisson equation

$$\nabla^2 \phi(\boldsymbol{r}, R) = -4\pi e[n_e(\boldsymbol{r}, R) - n_i(\boldsymbol{r}, R)]. \tag{6}$$

By definition the surface tension is

$$\gamma = \frac{1}{A}\left\{F[n_e(\boldsymbol{r}, R), n_i(\boldsymbol{r}, R)] - F[\bar{n}_e\theta(r-R), \bar{n}_i\theta(r-R)]\right\} \tag{7}$$

where $A = 4\pi R^2$ is the area of 'equimolecular' surface, $\bar{n}_e = \bar{n}_i \equiv \bar{n}$ is the charge concentration in the bulk, and $\theta(x)$ is the unit step function.

In order to employ the equations for a planar surface to describe spherical geometry it is convenient to expand n_a, ϕ, μ and γ in powers of the inverse radius $1/R$ of the cluster, i.e., $n_a = n_{a0} + n_{a1}/R$, $\phi = \phi_0 + \phi_1/R$, and so on. Then we may introduce the definition of the 'average over a flat surface':

$$\langle\mu_a(x)\rangle = -\frac{1}{\bar{n}_0}\int_{-\infty}^{\infty} \mathrm{d}x\ \mu_a(x)\ \frac{\mathrm{d}}{\mathrm{d}x}n_{a0}(x) \tag{8}$$

where we have changed the variable: $x = r - R$, and we have made use of the limit $R \to \infty$. Following [9, 17], from the zero-pressure condition for a planar surface, $P_0 = 0$, and from the condition of mechanical equilibrium for the electron and ion components, we obtain the following for a planar surface:

$$\bar{\mu}_{a0} = \pm e\bar{\phi}_0 + \bar{f}'_a \tag{9}$$

where the plus and minus signs correspond to $a = \mathrm{e}$ and $a = \mathrm{i}$, respectively,

$$\langle\mu_{e0}\rangle + \langle\mu_{i0}\rangle = \bar{f}_0/\bar{n}_0 \tag{10}$$

$$\gamma_0 = 2\int_{-\infty}^{\infty}\mathrm{d}x\ \left(f_{ee}\,|\nabla n_e|^2 + f_{ei}\nabla n_e\nabla n_i + f_{ii}\,|\nabla n_i|^2\right) - \frac{1}{4\pi}\int_{-\infty}^{\infty}\mathrm{d}x\ (\nabla\phi_0)^2 \tag{11}$$

and for the curvature corrections:

$$\bar{\mu}_{e1} = +e\bar{\phi}_1 + \bar{n}_{e1}\bar{f}''_{ee} + \bar{n}_{i1}\bar{f}''_{ei} \tag{12}$$

$$\bar{\mu}_{i1} = -e\bar{\phi}_1 + \bar{n}_{i1}\bar{f}''_{ii} + \bar{n}_{e1}\bar{f}''_{ei} \tag{13}$$

$$\langle\mu_{e1}\rangle + \langle\mu_{i1}\rangle = \frac{2\gamma_0}{\bar{n}_0} \tag{14}$$

$$\bar{\phi}_1 = 2\int_{-\infty}^{\infty}\mathrm{d}x\ \left[\phi_0(x) - \bar{\phi}_0\theta(-x)\right] + 4\pi e\int_{-\infty}^{\infty}\mathrm{d}x\ x\,[n_{e1}(x) - n_{i1}(x)]\,. \tag{15}$$

The explicit derivation of the latter equality is given in appendix A. In the derivation of equation (14) we have made use of equation (11). All of the quantities denoted by a bar above them are taken in the cluster centre (that is for $x \to -\infty$). For explicit density profiles, $\langle\mu\rangle$ must be equal to $\bar{\mu}$ and $\bar{f}_0 \equiv f(\bar{n}_{e0}, \bar{n}_{i0}, r_{c0})$ is the free energy per unit volume for uniform two-component plasma. Here, r_{c0} denotes the core radius of the pseudopotential that is used to describe the electron–ion interaction. The primes denote derivatives with respect to $\bar{n}_{a0}$ where $a = \mathrm{e}, \mathrm{i}$: $\bar{f}'_a = \partial\bar{f}_0/\partial\bar{n}_{a0}$, $\bar{f}''_{aa} = \partial^2\bar{f}_0/\partial\bar{n}^2_{a0}$ and $\bar{f}''_{ei} = \partial^2\bar{f}_0/\partial\bar{n}_{e0}\,\partial\bar{n}_{i0}$.

The sum of second derivatives gives the bulk modulus:

$$B_0 = \bar{n}_0^2\left(\bar{f}''_{ee} + 2\bar{f}''_{ei} + \bar{f}''_{ii}\right). \tag{16}$$

Note that the derivatives must be taken in a frozen-core approximation, $r_{c0} =$ constant. Combining equations (12)–(14), using the charge neutrality condition [17] and equation (16), we derive an explicit equality connecting the component concentration, surface tension, and bulk modulus:

$$\bar{n}_{e1} = \bar{n}_{i1} = 2\bar{n}_0\gamma_0/B_0. \tag{17}$$

This means that the component concentrations in the bulk of the cluster increase by $\bar{n}_{e1}/R$ compared to the case where $R \to \infty$. Thus, self-compression is a result of surface curvature which creates the extra pressure, $2\gamma/R$, in comparison to the planar surface case.

Let us write the quantities μ_{a1} and $\bar{\phi}_1$ in the form of the sums ($a = \mathrm{e}, \mathrm{i}$)

$$\mu_{a1} = \mu_{a1}^{rig} + \delta\mu_{a1} \tag{18}$$

$$\bar{\phi}_1 = \bar{\phi}_1^{rig} + \delta\bar{\phi}_1 \tag{19}$$

where the first terms appearing on the right-hand sides (r.h.s.) of equations (18) and (19) correspond to a rigid cluster. For such a hypothetical, liquid cluster we have

$$n_{a1}^{rig}(-\infty) \equiv \bar{n}_{a1}^{rig} = 0$$

and following (12) and (13) one gets

$$\mu_{a1}^{rig} = \pm e\bar{\phi}_1^{rig} \tag{20}$$

where

$$\bar{\phi}_1^{rig} = 2\int_{-\infty}^{\infty} \mathrm{d}x \ \left[\phi_0(x) - \bar{\phi}_0\theta(-x)\right] + 4\pi e \int_{-\infty}^{\infty} \mathrm{d}x \ x\left[n_{e1}^{rig}(x) - n_{i1}^{rig}(x)\right]. \tag{21}$$

Consequently, for rigid clusters in the framework of a two-component description and because $\bar{\mu}_{a1} = \langle\mu_{a1}\rangle$, equations (12) and (13) reduce to

$$\mu_{e1}^{rig} + \mu_{i1}^{rig} = 0. \tag{22}$$

On the other hand, from equations (14), (18), and (23), the 'self-compression' sum rule follows:

$$\delta\mu_{e1} + \delta\mu_{i1} = \frac{2\gamma_0}{\bar{n}_0}. \tag{23}$$

The term $-2\gamma_0/(\bar{n}_0 R)$ defines the size correction to the cohesive energy for zero temperature.

The non-electrostatic terms on the r.h.s. of equations (12) and (13) may be easily calculated, using the exact result (17). However, to determine $\bar{\phi}_1$ given by equation (15), it is necessary to solve entirely the problem of equilibrium electronic and ionic profiles for a self-compressed metallic cluster. This can be circumvented by calculating $\delta\bar{\phi}_1$ from the asymptotic expansion for $\bar{\phi}(R)$ in powers of the difference $\bar{n}_e(R) - \bar{n}_{e0} = \bar{n}_{e1}/R$. Leaving only the first-order terms we have

$$\bar{\phi}(R) = \bar{\phi}_0 + \frac{\delta\bar{\phi}_1}{R} = \bar{\phi}_0 + \bar{\phi}_0'\frac{\bar{n}_{e1}}{R} \tag{24}$$

where $\bar{\phi}_0' = \mathrm{d}\bar{\phi}_0/\mathrm{d}\bar{n}$ is calculated in each case with $\bar{n} = \bar{n}_0$ and for constant r_c. Using equations (17), (19), and (24), one can extract from equations (12) and (13) the self-compression parts to get

$$\delta\mu_{e1} = \frac{2\gamma_0}{\bar{n}_0}\left[1 - \frac{\bar{n}_0^2\left(\bar{f}_{ii}'' + \bar{f}_{ei}'' - e\bar{\phi}_0'\right)}{B_0}\right] \tag{25}$$

and

$$\delta\mu_{i1} = \frac{2\gamma_0}{\bar{n}_0}\left[1 - \frac{\bar{n}_0^2\left(\bar{f}_{ee}'' + \bar{f}_{ei}'' + e\bar{\phi}_0'\right)}{B_0}\right]. \tag{26}$$

It can be seen that these expressions allow the effects of self-compression on the IP and EA of clusters to be predicted from these quantities for a liquid metal with a flat surface.

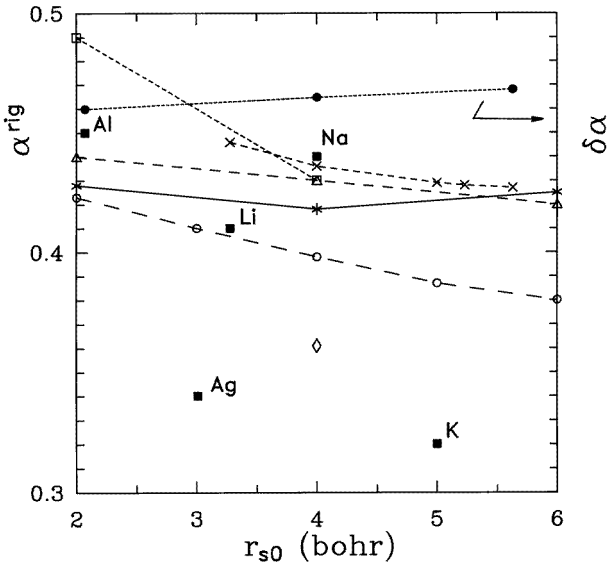

Figure 1. The values of $\alpha^{rig} = \frac{1}{2} - \mu_{e1}^{rig}$ (see the text) calculated within different approaches for rigid and cold clusters of simple metals: □, [7]; ◊, [8]; ×, [9]; ∗, [10]; △, [11]; ○, [12]. They are compared with the experimental data (■, [3]) and the present stabilized-jellium estimation (●) of $\delta\alpha = \frac{1}{2} - \delta\mu_{e1}$ (right-hand scale).

2.2. The stabilized-jellium model

In the framework of a stabilized-jellium (one-component) model, using our results [17] for large clusters, and taking into account their self-compression, we have

$$\mu_{e1} = \bar{\phi}_{e1} + \bar{n}_{e1}\left[\bar{n}_0\bar{\varepsilon}_0'' + \bar{\varepsilon}_{j0}'\right] \tag{27}$$

where $\bar{\varepsilon}_0 = \bar{\varepsilon}_{j0} + \Delta\bar{\varepsilon}_0$, where $\bar{\varepsilon}_0$ and $\bar{\varepsilon}_{j0}$ are the average energies per electron for the stabilized jellium and ordinary jellium respectively. Here $\Delta\bar{\varepsilon}_0$ is a sum of the Madelung energy of a point ion embedded in a uniform negative charge background and the Ashcroft pseudopotential averaged over the spherical Wigner–Seitz cell. Note that the band-structure energy is neglected in these expressions. For the explicit form, cf. [15] or [17]. The primes denote the derivatives taken with respect to $\bar{n}_0$. For this model, in equations (6) and (15) the substitutions

$$n_{i0}(x) \to \bar{n}_0\theta(-x) \qquad \text{and} \qquad n_{i1}(x) \to \bar{n}_{e1}\theta(-x)$$

are made, because the ionic background is a step function. In this case one can write for $\delta\mu_{e1}$ a formula similar to (25) and (26):

$$\delta\mu_{e1} = \frac{2\sigma_0}{\bar{n}_0}\left[1 + \frac{\bar{n}_0^2\left(\bar{\varepsilon}_{j0}' + e\bar{\phi}_0'\right)}{B_0}\right] \tag{28}$$

where σ_0 is surface energy, and the bulk modulus $B_0 = \bar{n}_0^3\bar{\varepsilon}_0''$. Thus, we have derived a simple expression for $\delta\mu_{e1}$ which applies to solid clusters of simple metals.

3. Results and discussion

At this point it is convenient for the purposes of the following discussion and to enable a comparison to be made with previous rigid-cluster computations to introduce the notation

$$\alpha^{rig} = \frac{1}{2} - \frac{\mu_{e1}^{rig}}{e^2} = \frac{1}{2} - \frac{\bar{\phi}_1^{rig}}{e^2}$$
$$\delta\alpha = \frac{1}{2} - \frac{\delta\mu_{e1}}{e^2}.$$

In figure 1 we have plotted the values of the coefficient α^{rig} calculated for zero temperature by different authors [7–12]. They are compared with the available experimental data [3]. Calculations for rigid clusters performed using the ordinary jellium model indicate the increase of electron density to spill out beyond the spherical boundary with the growth of its curvature. This infers that the bottom of the potential, $\bar{\phi}^{rig}(R) < 0$, becomes more positive with the decrease of R—that is, $\bar{\phi}_1^{rig} > 0$. As can be observed from figure 1, most of the calculations show that α^{rig} decreases with increase of r_{s0}. On the other hand the experimental data for α are very scattered and do not show any regular trend. A possible reason of this is the dependence of the IP on the cluster temperature, and the effect of compression under surface tension.

Table 1. The quantities (in atomic units) extracted from the Kohn–Sham calculation for the planar surface of stabilized jellium and the results for the correction to the electron chemical potential $\delta\mu_{e1}$. σ_0 is the surface energy (1 dyn cm^{-1} = 6.42×10^{-7} au), $\bar{\varepsilon}'_{j0}$ is the derivative of the bulk energy of jellium, $\bar{\phi}'_0$ is the derivative of the surface dipole barrier, and B_0 is the bulk modulus (1 Mbar = 3.41×10^{-3} au).

Metal	r_{s0}	T (K)	$(2\sigma_0/\bar{n}_0) \times 10^2$	$\bar{\varepsilon}'_{j0}$	$-\bar{\phi}'_0$	$B_0 \times 10^4$	$\delta\mu_{e1} \times 10^2$
Al	2.055	0	4.3789	3.3961	4.0550	57.210	3.997
	2.070	300	4.4152	3.3977	4.0836	53.608	4.006
	2.078	466.5	4.4349	3.3984	4.0995	51.718	4.010
	2.101	933*	4.4889	3.3999	4.1441	46.806	4.017
Na	3.906	0	5.8671	0.8487	7.5970	2.978	3.733
	3.959	186	5.8717	0.6906	7.6953	2.635	3.562
	3.990	293	5.8739	0.5975	7.5536	2.458	3.526
	4.012	371*	5.8754	0.5286	7.7918	2.337	3.382
Cs	5.580	0	5.7718	−6.4471	10.6341	0.730	3.223
	5.630	92	5.7646	−6.7421	10.0111	0.674	3.200
	5.662	150.5	5.7600	−6.9319	10.7677	0.640	3.006
	5.744	301*	5.7478	−7.4288	10.9020	0.562	2.776

* The melting temperature, T_m.

3.1. The stabilized-jellium model

Consider the solid clusters first. As we have shown—equation (28)—the effect of self-compression can be estimated using the results for a planar surface of stabilized jellium. It is well known from density functional calculations that for simple metals the surface dipole barrier $\bar{\phi}_0$ is monotonic function of r_{s0} or $\bar{n}_0$. Therefore in order to determine the derivative $\bar{\phi}'_0 = \mathrm{d}\bar{\phi}/\mathrm{d}\bar{n}_0$ appearing in equation (28) we may use the results of the Kohn–Sham calculations for a planar surface performed earlier by one of us [14, 15]. By numerical

fitting, the dependence $\bar{\phi}_0(\bar{n}_0)$ can be obtained for the whole metallic density range. In this work, however, we have found that $\bar{\phi}_0'$ is determined more accurately by direct numerical calculation of the derivative of the surface dipole barrier for the density corresponding to a given metal. As a result, for every metal we have performed two additional calculations: one for slightly higher density (r_s), and one for slightly lower density. The $\bar{\phi}_0'$ calculated in this way and the other quantities appearing in (28) which were used in the calculation of $\delta\mu_{e1}$ are listed in table 1. As is seen, the values of $\delta\mu_{e1}$ calculated in the stabilized-jellium model for Al, Na, and Cs are very close each to the other (the difference between the values for Al and Cs does not exceed 0.008). They are of magnitude comparable to that of the previous calculations of $\frac{1}{2} - \alpha^{rig}$ (see figure 1). This means that self-compression has a noticeable influence upon the IP and EA of cold clusters, decreasing the size corrections predicted by the rigid-cluster calculations. This conclusion is in accordance with the results of Perdew *et al* [16] for Al clusters, but their $\delta\mu_1$ (denoted as Δc) was found to be negligible for Na and Cs. Montag *et al* [24], using a structure-averaged-jellium model, reported that the compression gives a sizeable effect for all sorts of metallic clusters, being largest for the densest metals.

Table 1 shows also the temperature dependence of $\delta\mu_{e1}$. For aluminium $\delta\mu_{e1}$ increases with temperature, whereas for Na and Cs the opposite effect is observed. This behaviour of $\delta\mu_{e1}$ is determined by the interplay between the $\bar{\varepsilon}_{j0}'$- and $\bar{\phi}_0'$-terms in equation (28). Note that the bulk modulus B_0 is a decreasing function of temperature.

Table 2. The temperature dependence of the work functions for the flat surfaces of simple metals represented by the stabilized-jellium model. λ is the linear thermal expansion coefficient. W_{e0} is the work function.

Metal	r_{s0}	T_1 (K)	λ (K^{-1})	T (K)	W_{e0} (eV)
Al	2.07	300	24×10^{-6}		
	2.055			0	4.276
	2.078			466.5	4.259
	2.101			933*	4.241
Na	3.99	293	7.2×10^{-5}		
	3.906			0	2.983
	3.959			186	2.949
	4.012			371*	2.924
Cs	5.63	92	9.7×10^{-5}		
	5.580			0	2.264
	5.662			150.5	2.241
	5.744			301*	2.212

* The melting temperature, T_m.

To discuss the effect of temperature it is useful to consider the temperature dependence of the electron work function for a planar surface, which enters the definitions (1) for the IP and EA of clusters. We have performed the stabilized-jellium calculation of the work function for three different metals (Al, Na, and Cs) at the temperatures $T = 0$, $T_m/2$, and T_m, where T_m is the melting temperature. In the stabilized-jellium model the work function depends only on the average electron concentration in the metal interior (or on the density parameter r_s). A simple temperature-independent linear coefficient of thermal expansion, λ, for the Wigner–Seitz radius has been assumed thus:

$$r_s = r_{s0}[1 + \lambda(T - T_1)].$$

Note that now the pseudopotential core radius r_c is determined for r_s corresponding to a

given temperature, i.e., r_s is treated as a material parameter. The results are summarized in table 2. For Al surfaces the temperature gradient of the work function is negative and equals -3.8×10^{-5} eV K^{-1}. For Na and Cs it is also negative, and is larger. For Na surfaces it equals -1.8×10^{-4} to -1.4×10^{-4} eV K^{-1} and for Cs it equals -1.5×10^{-4} to -1.9×10^{-4} eV K^{-1}. Note that for ordinary jellium the temperature derivative of the work function is negative and of the same order of magnitude [18].

Comparing the results of tables 1 and 2 we see that for Al clusters the size effect of $\delta\mu_{e1}$ may compensate the effect of temperature on W_{e0} and thus the IP will stay constant. For Na and Cs both the IP and W_{e0} decrease with temperature.

3.2. The two-component model

In the second step we have estimated the influence of self-compression on the IP and EA for *hot* and *liquid* clusters using the equations of the previous section. To this end the temperature dependences of γ_0, $W_e(T)$, and $\bar{\phi}_0(T)$ were computed for the concentration $\bar{n}_e$ of Na and Cs at the saturation line, following the approach of [20]. (The input parameters for liquid Al were not available to us.)

The exact numerical solution of the system of the Euler–Lagrange equations, or the evolution of the minimum of the functional $F[n_{e0}(x), n_{i0}(x)]$ and calculation of the optimum distributions $n_{e0}(x)$ and $n_{i0}(x)$, is quite complicated. Therefore, we have employed the direct variational method with the one-parameter trial functions

$$n_{e0}(x) = \bar{n}_0/(1 + \mathrm{e}^{x/L}) = \bar{n}_0 \sum_{k=0}^{\infty} (-1)^k \mathrm{e}^{bx/L} \tag{29}$$

where $b = k$ for $x < 0$, and $b = -(k+1)$ for $x > 0$, for the electron distribution, and

$$n_{i0}(x) = \bar{n}_0/(1 + \mathrm{e}^{x/M}) \tag{30}$$

for the ion concentration. The of parameters L and M are optimized by determining the global minimum of $\gamma_0(L, M)$ for every temperature. Since the minimum of $\gamma_0(L, M)$ is very shallow, the accuracy of the calculation was checked by determining L and M using equation (13). The details of the calculational procedure are given in [20].

Table 3. The calculated electron work functions for flat surfaces of liquid Na and Cs in the two-component model.

		Work function (eV)		
Metal	Temperature	This work	Theory [20]	Experiment
Na	T_m	2.06	1.72	2.39[a]
	450			2.32[a]
	600	1.85	1.42	
	1000	1.52	0.86	
Cs	0			1.81[b]
	T_m	1.58	1.31	
	600	1.32	1.00	
	1000	0.87	0.51	

[a] Alchagirov *et al* [25].
[b] Fomenko and Podchernyaeva [26].

Our results for γ_0 agree quite well with the calculations performed in [20] where another form of the trial function was used. The electron work function for a semi-infinite liquid

metal was obtained via definition (8). At the triple point (see table 3), the calculated values of W_{e0} are 10–20% lower than the measured ones [25, 26]. The decrease in $W_{e0}(T)$ was found to be weaker than that calculated in [20]. These values are sensitive to the choice of trial functions.

Table 4. The input data and results for the size-compression correction to the chemical potential of liquid clusters calculated from equation (26) and (27). For each metal three different temperatures were considered: $T = T_m$, 600 K, 1000 K (ordered from the top to the bottom).

Metal	r_{s0}	$(2\gamma_0/\bar{n}_0)$ $\times 10^2$	$\bar{f}''_{ee}$	$-\bar{f}''_{ii}$	$\bar{f}''_{ei}$	$-\bar{\phi}'_0$	$B_0 \times 10^2$ Calc.	$B_0 \times 10^2$ Exp. [27]	$\delta\mu_{e1}$	$\delta\mu_{i1}$
Na	4.048	5.93	7.218	17.279	15.144	9.27	2.619	1.835	3.84	2.09
	4.129	5.30	8.011	24.448	14.740	11.0	1.499	1.438	4.67	0.63
	4.292	4.03	9.452	34.007	14.051	15.3	0.324	1.074	9.34	−5.31
Cs	5.785	8.30	19.401	32.442	23.584	6.20	0.518	0.494	8.66	−0.62
	5.975	7.37	24.463	53.571	26.390	6.41	0.296	0.345	13.8	−6.47
	6.276	5.65	31.218	81.667	30.471	7.50	0.0979	0.198	29.2	−23.5

The magnitude of $\delta\phi_1$ is evaluated by use of $\Delta\bar{\phi}_0/\Delta\bar{n}$, where $\Delta\bar{n} = \pm 0.01\bar{n}_0$, for every estimated temperature. The results of calculations are displayed in table 4 where the curvature correction of equations (26) and (27) is decomposed into the individual contributions. These are relatively large, and tend to cancel each other. The orders of magnitude of γ_0, $\bar{\phi}'_0$, B_0 and $\delta\mu_{e1}$ estimated within the two-component description agree with the corresponding quantities given in table 1.

The calculations of bulk modulus at high temperatures are performed here, as far as we are aware, for the first time. At the triple point and at $T = 600$ K the calculated values of B_0 agree reasonably well with the experimental ones [27], but at $T = 1000$ K there are considerable deviations. Possible reasons for this are as follows.

(i) The using of the frozen pseudopotential radii in a variational procedure, $r_c(T) = 1.90$ and $3.215a_0$ for Na and Cs respectively. (Nevertheless, a detailed analysis in [20] gave $r_c = 1.84(T_m)$ and 1.96(1000 K) for sodium which is not much different to the values employed by us.)

(ii) The neglect of fourth-order gradient terms in the energy.

(iii) A strengthening of the role of electron correlations in the screening of the ion–ion interaction at high temperatures. The form of the band-structure energy, which in general describes this interaction, depends on the Fourier transform of the screened ion–ion interaction and the Percus–Yevick hard-sphere structure factor for a fluid [28]. This term gives a considerable contribution to B_0 as was noticed earlier. Following the model of [29] we have neglected it in f''_{ii}, but it was taken into account in f''_{ee} and f''_{ei}.

As is seen from table 4, the results for $\delta\mu_{e1}(T)$ calculated in the framework of this approach show a strong increasing tendency with the increased temperature which contradicts the trend observed by us for solid clusters of these metals (compare table 1). This leads to the decrease of the value of α. It is also seen that our data for $\delta\mu_{e1}(T)$ and $\delta\mu_{i1}(T)$ are modelled very well by the self-compression sum rule (23). Further study is needed to resolve whether for Na and Cs the effect is real or whether it is a consequence of using two different models which may be inconsistent.

3.3. The effect on the static polarizability

The size shrinkage can be also introduced into the theory of static polarizability and the shift of the surface plasma resonance of closed-shell clusters. The influence of self-compression on the static polarizability, α_s, of a spherical cluster can be estimated in a simple way. Following the density functional analysis of Snider and Sorbello [30], the polarizability, α_s^{rig}, of a large rigid cluster of radius $R^{rig} = r_{s0}N^{1/3}$, where $N \equiv N_e$, can be expressed as

$$\alpha_s^{rig} = (R^{rig} + \delta_s)^3 \tag{31}$$

where $\delta_s = x_0 + \mathrm{O}(1/R)$, in the limit $R \to \infty$, gives the position x_0 of the centre of mass of the charge which is induced at the planar surface [31] by a weak external electric field.

We can write an analogous formula for the polarizability when the self-compression occurs. By expressing the cluster radius in the form $R = r_s N^{1/3}$ and taking into account that the difference between r_s and r_{s0} is given [17] by the ratio $r_s/r_{s0} = (1+2\sigma_0/(B_0R))^{-1/3}$, we obtain

$$\alpha_s(N) = Nr_{s0}^3(1 + \Delta/N^{1/3}) \tag{32}$$

where $\Delta = (3x_0 - 2\sigma_0/B_0)/r_{s0}$. Simple estimates for stabilized jellium are $\Delta = 0.94$, 0.82, 0.73, and 0.66 for solid Al, Li, Na, and K, respectively, and demonstrate that self-compression compensates the size dependence of the polarizability by 50%, approximately. Unfortunately, the values of $\alpha_s(N)$ have been measured for small clusters of K, Na, and Al (see, for example, [3]), and our theoretical dependencies describe experimental data only qualitatively.

Assuming that all of the dipole oscillator strength is exhausted by the surface plasma resonance at ω_r, we can estimate it in terms of α_s, as has been suggested by Lushnikov *et al* [32]:

$$\omega_r = (N/\alpha_s(N))^{1/2}.$$

Here the dependence $\alpha_s(N)$ corrects the classical Mie frequency $\omega_{Mie} = \omega_p/\sqrt{3}$, where ω_p is the bulk plasma frequency, via a factor $\omega_r/\omega_{Mie} = 1 - \Delta/2N^{1/3}$. Thus, as was remarked by Kreibig and Genzel [33], self-compression leads to a weakening of the red-shift tendency for the plasmon peak position. A shift of the surface plasmon peak to lower frequencies (red-shift), as the cluster size decreased, was investigated experimentally by Brechignac *et al* [34, 35]. The experiments were performed for large clusters of K_N^+ (for $N = 500$, 900) and Li_N^+ (in the size range up to $N = 1500$). For these values of N one can neglect the effect of electrostriction in the estimation of ω_r. However, taking into account the experimental error (± 0.05 eV) and the temperature of the clusters (about 700 K), which may contribute to a shift $\sim$0.06 eV, it is difficult to draw any firm conclusions about a role of self-compression in these experiments.

4. Summary and conclusions

The clusters prepared in supersonic expansion experiments are most probably in a hot environment or even in a liquid-like state [2, 3]. In this paper we have studied the effect of temperature-dependent size shrinkage on the ionization potentials of solid and liquid clusters. We have derived the analytical expressions and sum rules for clusters. They allow the compression corrections to be calculated from data for flat surfaces. We have employed two models: a stabilized-jellium model for solid clusters; and a two-component plasma model for the liquid case.

We have reported self-consistent Kohn–Sham results for the temperature-dependent work function of a planar surface of stabilized jellium. The temperature derivative of the work function is found to be negative for all of the metals considered. Our calculations have shown that temperature-dependent self-compression has a significant effect on the ionization potentials and the electron affinities of solid- and liquid-metal clusters. Consequently it is essential that these effects are included in any analysis of measured data. We have calculated the bulk modulus of liquid alkali metals, which is found to be in reasonable agreement with measured values. The temperature dependence of $\mu_{e1}^{rig}(T)$ is beyond the scope of our investigation, and awaits further study in the future.

Finally, using our numerical results we have analysed the influence of size shrinkage on the static polarizability and on the shift of the plasmon resonance peak. It is shown that simple estimates that take these effects into account can provide some insight into the physics behind the measured trends for real clusters.

Acknowledgments

The work of AK was supported by the University of Wrocław under the grant 1010/S/IFD/96; that of VVP was supported by the Russian Foundation for Basic Research.

Appendix A. The explicit expression for $\bar{\phi}_1$

We start from the Poisson equation (6) with boundary conditions for $r > R$:

$$\lim_{r\to\infty} \phi(r, R) = 0 \qquad \lim_{r\to\infty} \mathrm{d}\phi(r, R)/\mathrm{d}r = 0.$$

After expansion of the electrostatic potential in powers of the inverse cluster radius $1/R$ and making the change of variable $x = r - R$, in the limit $R \to \infty$, we obtain the first two equations of the hierarchy:

$$\frac{\mathrm{d}^2\phi_0(x)}{\mathrm{d}x^2} = -4\pi e\,[n_{e0}(x) - n_{i0}(x)] \tag{A.1}$$

$$\frac{\mathrm{d}^2\phi_1(x)}{\mathrm{d}x^2} + 2\frac{\mathrm{d}\phi_0(x)}{\mathrm{d}x} = -4\pi e\,[n_{e1}(x) - n_{i1}(x)] \tag{A.2}$$

with the boundary conditions $\phi_{0,1}(+\infty) = 0$ and $\mathrm{d}\phi_{0,1}(x)/\mathrm{d}x|_{x=+\infty} = 0$.

Integration of (A.2) from x to ∞ yields

$$\phi_0(x) = 2\int_x^\infty \mathrm{d}x'\ \phi_0(x') - 4\pi e\int_x^\infty \mathrm{d}x' \int_{x'}^\infty \mathrm{d}x''\ \left[n_{e1}(x'') - n_{i1}(x'')\right]. \tag{A.3}$$

Performing integration by parts for the last term in (A.3) and setting $x = 0$, we have

$$\phi_1(0) = 2\int_0^\infty \mathrm{d}x\ \phi_0(x) + 4\pi e\int_0^\infty \mathrm{d}x\ x\,[n_{e1}(x) - n_{i1}(x)]. \tag{A.4}$$

On the other hand, by integrating (A.2) in the range $-\infty, x$ and setting $x = 0$, one can write

$$\bar{\phi}_1 - \phi_1(0) = 2\int_{-\infty}^0 \mathrm{d}x\ \left[\phi_0(x) - \bar{\phi}_0\right] + 4\pi e\int_{-\infty}^0 \mathrm{d}x\ x\,[n_{e1}(x) - n_{i1}(x)]. \tag{A.5}$$

Combining (A.5) and (A.4), we finally arrive at equation (15).

References

[1] Halperin W P 1986 *Rev. Mod. Phys.* **58** 533
[2] Kappes M M and Schumacher E J 1988 *Z. Phys. Chem., NF* **156** 23
[3] de Heer W A 1993 *Rev. Mod. Phys.* **65** 611
[4] Nagaev E L 1992 *Phys. Rep.* **222** 201
[5] Brack M 1993 *Rev. Mod. Phys.* **65** 677
[6] Seidl M and Perdew J P 1994 *Phys. Rev.* B **50** 5744
[7] Snider D R and Sorbello R S 1983 *Solid State Commun.* **47** 845
[8] Rubio A, Balbas L C and Alonso J A 1990 *Physica* B **167** 19
[9] Pogosov V V 1990 *Solid State Commun.* **75** 469
[10] Engel E and Perdew J P 1991 *Phys. Rev.* B **43** 1331
[11] Makov G and Nitzan A 1991 *J. Chem. Phys.* **95** 9024
[12] Seidl M, Meiwes-Broer K H and Brack M 1991 *J. Chem. Phys.* **95** 1295
[13] Perdew J P, Tran H Q and Smith E D 1990 *Phys. Rev.* B **42** 11 627
[14] Kiejna A 1993 *Phys. Rev.* B **47** 7361
[15] Kiejna A, Ziesche P and Kaschner R 1993 *Phys. Rev.* B **48** 4811
[16] Perdew J P, Brajczewska M and Fiolhais C 1993 *Solid State Commun.* **88** 795
[17] Iakubov I T and Pogosov V V 1995 *Physica* A **214** 287
[18] Kiejna A 1986 *Surf. Sci.* **178** 349
[19] Wood D M and Stroud D 1983 *Phys. Rev.* B **28** 4374
[20] Iakubov I T, Khrapak A G, Pogosov V V and Trigger S A 1985 *Solid State Commun.* **56** 709
[21] Rubio A, Balbas L C and Alonso J A 1991 *Z. Phys.* D **19** 93
[22] Genzken O and Brack M 1991 *Phys. Rev. Lett.* **67** 3286
[23] Pogosov V V 1994 *Solid State Commun.* **89** 1017
[24] Montag B, Reinhard P-G and Meyer J 1994 *Z. Phys.* D **32** 125
[25] Alchagirov B B, Arkhestov Z Kh and Khokonov Kh B 1993 *Zh. Fiz. Chim.* **67** 1892
[26] Fomenko V S and Podchernyaeva J A 1975 *Emission Properties of Materials* (Moscow: Atomizdat) (in Russian)
[27] Trelin Yu S 1981 *Dr Sci. Thesis* Moscow Institute of Engineering Physics
[28] Ashcroft N W and Stroud D 1978 *Solid State Physics* vol 33 (New York: Academic) p 1
[29] Hasegawa M and Watabe M 1972 *J. Phys. Soc. Japan* **32** 14
[30] Snider D R and Sorbello R S 1983 *Phys. Rev.* B **28** 5702
[31] Kiejna A 1995 *Surf. Sci.* **331–333** 1167
[32] Lushnikov A A, Maksimenko V V and Simonov A J 1982 *Electromagnetic Surface Modes* ed A D Boardman (New York: Wiley) p 305
[33] Kreibig U and Genzel L 1985 *Surf. Sci.* **156** 678
[34] Brechignac C, Cahuzac P, Kebaili N, Leygnier J and Sarfati A 1992 *Phys. Rev. Lett.* **68** 3916
[35] Brechignac C, Cahuzac P, Leygnier J and Sarfati A 1993 *Phys. Rev. Lett.* **70** 2036